CrystEngComm

RSC Publishing

PAPER

View Article Online
View Journal | View Issue

Nanoparticle-based crystal growth *via* multistep self-assembly

Cite this: *CrystEngComm*, 2013, **15**, 5114

Qiang Zhou,[a] Boyang Wang,[b] Peijie Wang,[a] Christoph Dellago,[c] Yanting Wang*[b] and Yan Fang*[a]

Received 20th March 2013,
Accepted 15th April 2013

DOI: 10.1039/c3ce40497h

www.rsc.org/crystengcomm

Metal crystals are assumed to form through a combined process of Ostwald ripening and oriented attachment. Our experiments and simulations, however, indicate that metal crystals are grown in a multistep self-assembly process with metal nanoparticles as basic building blocks. The shapes of the intermediate dendritic structures are determined by the geometric and energetic features of the nanoparticles.

Introduction

Crystal growth is at the very heart of various research fields ranging from surface physics, crystallography, materials science, and biological structure determination to semiconductor technology and computer chip manufacturing.[1–4] Understanding the original processes of crystal formation is very important to the control of crystal growth activities. Conventional crystal growth theories generally postulate that crystals grow by addition of individual atoms or ions into an interfacial region.[5–8] For instance, Frank[9,10] pointed out that close to equilibrium perfect crystals grow only very slowly due to high nucleation barriers and Burton and Cabrera proposed that crystal surfaces grow stepwise either laterally or in the normal direction.[11–15] These theories work particularly well when the system is near equilibrium, but would not apply to crystal growth far from equilibrium.[16,17]

Recently, Alivisatos *et al.*[18] have reported their experimental discovery that platinum nanocrystals can grow by both monomer attachment and particle coalescence, demonstrating the importance of particle–particle interactions during nanocrystal growth. In this paper, we report on experiments in which silver crystals are grown in a non-equilibrium process with nanoparticles, rather than individual atoms, as basic building blocks. Although some experiments[19–23] have previously observed dendritic structures of metals, no detailed microscopic mechanisms have been proposed to explain the self-assembly procedure of dendritic structure formation, and Ostwald ripening[24] combined with oriented attachment[25] was assumed to be able to explain the growth mechanism.

However, our current study discourages that assumption and reveals that the growth process is composed of three steps: 1) individual atoms aggregate locally to form nanoparticles through a fast process within seconds; 2) self-assembled intermediate dendritic structures occur within minutes; 3) the dendritic structures are filled up to form solid crystals in a couple of hours. Combining the results of experimental observations and molecular dynamics simulations, we propose a detailed mechanism which indicates that the shapes of the dendritic structures are determined by the geometric and energetic features of the nanoparticles.

Our proposed mechanism provides a deep insight into the formation of nanoscale metal dendritic structures *via* self-assembly and is helpful for understanding crystal growth dynamics with possible applications in the engineering of nanoscale crystals with new architectures. For example, protein nanoparticles could be obtained and manipulated during controlled protein crystal growth, and become the building blocks for highly ordered crystal biomolecular devices[26] with designed structures and functions. Furthermore, inorganic and organic nanoparticles could be assembled into complex patterns to form superfine crystal nanocircuits[27] for use in electronic circuits, or to manufacture extremely thin crystal tips for applications in high resolution microscopies[28] and other nanoscale machineries.

Experimental

Growth of Ag dendritic structures

A copper thin film was initially immersed in an $AgNO_3$ solution, and a replacement reaction took place on the copper surface. All chemical reagents in this experiment were of analytical grade and were used without further purification.

[a]*Beijing Key Laboratory for Nanophotonics and Nanostructure, Department of Physics, Capital Normal University, Beijing 100048, China. E-mail: yanfang@cnu.edu.cn*
[b]*State Key Laboratory of Theoretical Physics, Institute of Theoretical Physics, Chinese Academy of Sciences, Beijing 100190, China. E-mail: wangyt@itp.ac.cn*
[c]*Faculty of Physics and Center for Computational Materials Science, University of Vienna, Boltzmanngasse 5, A-1090 Vienna, Austria*

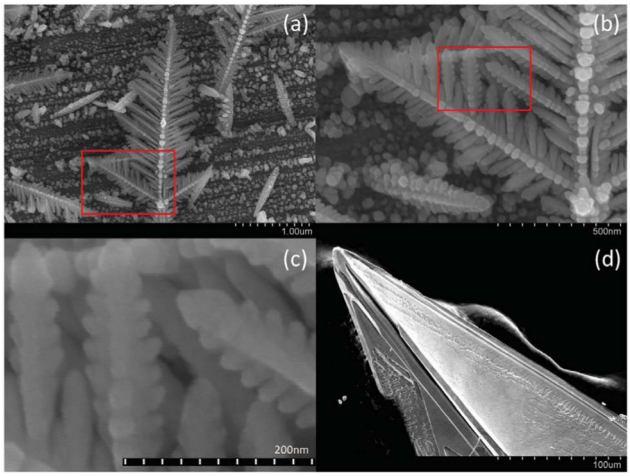

Fig. 1 Intermediate self-assembled silver dendritic structure after 30 s of reaction time (a) and silver crystal structure after 2 hours (d). The region marked by the red rectangle in (a) is enlarged in (b), and (c) further enlarges the red rectangle region in (b), indicating that the basic building blocks of the dendritic fractal structure are silver nanoparticles.

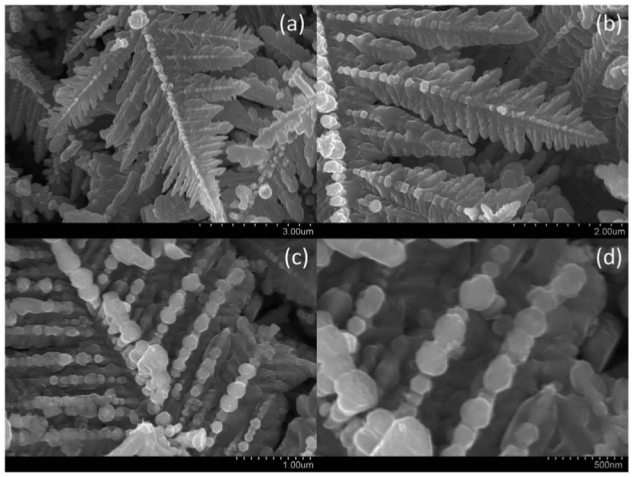

Fig. 2 Self-assembled dendritic structures of the silver crystal after 8 minutes of reaction time, viewed at different perspectives and resolutions.

The water was distilled twice before use. First, 0.4245 g of $AgNO_3$ was dissolved in 50 mL of distilled water and then a clean copper foil was dropped into this solution at room temperature (300 K) for 1 minute. Subsequently, the copper foil with gray precipitates was picked up and washed with distilled water several times. After the treatment, gray silver products were collected and dried at room temperature for 24 hours.

Results and discussion

Fig. 1a shows an electron micrograph of a dendritic structure formed after the reaction took place for 30 seconds. As can be seen in Fig. 1b and 1c, the structures of the side branches resemble those of the main branch. These pictures indicate that the dendritic fractal structure was hierarchically formed by the self-assembly of silver nanoparticles as basic building blocks. Fig. 2 shows the dendritic structure after 8 minutes of reaction time, viewed at different perspectives and resolutions. The side branches of the dendritic structure became less well defined at that time, because as the reaction went on, more silver deposited into the spaces between the side branches. The side branches were rounded and only the profiles of the largest side branches could still be identified. After 2 hours of reaction, the dendritic structures finally grew into thick ribbons shown in Fig. 1d. Individual silver nanoparticles can no longer be identified in these ribbons and their profiles are greatly smoothed out.

The selected-area electron diffraction (SAED) pattern of the dendritic structures demonstrates that they might be single crystals of silver. The left panel of Fig. 3 shows the results of X-Ray Diffraction (XRD) measurements of the dendritic crystal structures. The lattice constants determined from these XRD measurements are $a = b = c = 0.4081$ nm, very close to the standard value of 0.4077 nm for a silver crystal as obtained from the JCPDS04-0783 XRD database. The right panel of Fig. 3 shows the SAED pattern of the dendritic structures, demonstrating that they are very likely to be single crystals of silver. More delicate experiments, such as transmission electron microscopy, will be able to unambiguously conclude if they are truly single crystals, but it is beyond the central focus of this work.

In order to understand the detailed processes of the crystal growth by self-assembly, after the reaction had taken place for 8 minutes, we cut and peeled off several layers of silver formed on the surface of the copper substrate. The image of the silver layers is shown in the left panel of Fig. 4. It can be seen that the bottom layer on the copper surface is formed by randomly distributed discrete Ag nanoparticles. These nanoparticles have diameters of tens to hundreds of nanometers, as can be inferred from the enlarged image shown in the right panel of Fig. 4.

We suggest the following mechanism to explain the formation of the silver layers on the copper surface. After the Ag atoms are replaced out of the solution by Cu atoms due to the reduction reaction, they immediately aggregate locally to

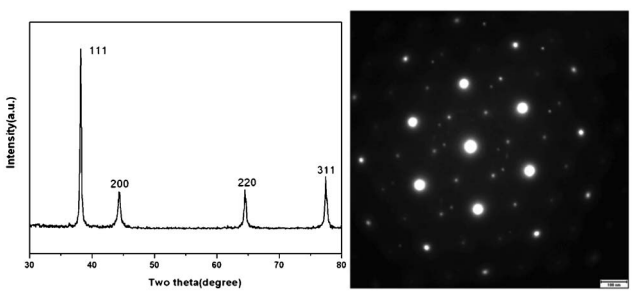

Fig. 3 (Left) Results of XRD measurements of the dendritic crystal samples. (Right) SAED pattern of the dendritic nanostructures, indicating that they might be single crystals of silver.

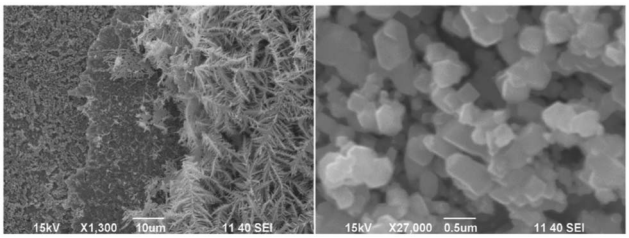

Fig. 4 (Left) Four different layers formed on the surface of the copper substrate after 8 minutes of reaction. From left to right: Ag nanoparticle layer, Ag film layer, smaller dendritic-structure layer, and larger dendritic-structure layer. (Right) Enlarged image of the first layer with Ag nanoparticles deposited on the copper surface.

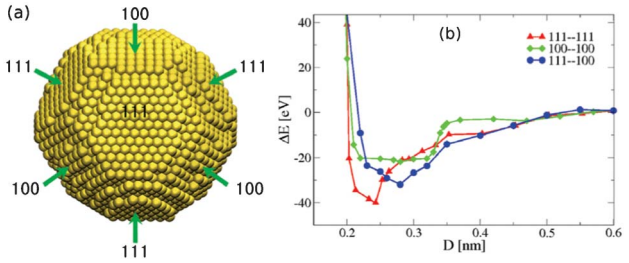

Fig. 5 (a) Simulated stable structure of a 6181-atom silver nanoparticle. (b) Total potential energy ΔE with respect to the energy at infinite separation of two 6181-atom nanoparticles with a truncated octahedral structure approaching each other in three orientations, *versus* the center-of-mass distance D between the two closest facets.

form Ag nanoparticles with center-of-mass positions randomly distributed in the whole space on or near the copper surface. Some silver nanoparticles deposit on the copper surface to form the first layer of silver thin film. More silver nanoparticles continue to deposit on the first layer to form the second layer of silver thin film. Possibly because silver nanoparticles are easier to attach on a silver surface than on a copper surface, the second layer is more compact than the first layer. Only on this compact silver thin film can the silver nanoparticles aggregate and self-assemble into small dendritic structures, forming the third layer. Silver nanoparticles which deposit on the third layer build up the fourth layer composed of larger dendritic structures. The structures in the fourth layer are larger, possibly because the reduction reaction mainly happens near the copper surface and fewer silver particles can arrive at the fourth layer.

In order to understand the growth mechanism and the resulting shape of the silver crystal, we performed molecular dynamics (MD) simulations to study the structure and energetics of silver nanoparticles, which, as basic building blocks, determine the crystal growth process. MD simulations were carried out using the DL_POLY software package[29] with the silver atoms modeled by the Sutton–Chen force field.[30] First, a simulated annealing[31] procedure was conducted for a single 6181-atom Ag nanoparticle in vacuum to find its stable crystal structure and shape. The temperature was first set to T = 1200 K, and then the system was cooled down step by step in intervals of 100 K to a temperature of T = 100 K. At each temperature, a 10 ns simulation was performed with a time step of 4.0 fs. In these simulations, a Nosé–Hoover thermostat[32,33] with a relaxation constant of 0.1 ps was used to keep the system at the selected temperature. Our MD simulations indicate that the most stable structure of a 6181-atom silver nanoparticle is a truncated octahedron, as shown in Fig. 5a. According to the theoretical calculations based on Ino's theory,[34,35] larger silver nanoparticles, such as those with diameters of 10–30 nm appearing in our experiments (see Fig. 6a), should also have a truncated octahedron structure.

To investigate the tendency of silver nanocrystals to self-assemble, we compute the interactions between two nanocrystals as a function of their distance. Since the surface of a truncated octahedron is covered by eight (111) facets and six (100) facets, two nanoparticles can approach each other with 3 possible facet–facet combinations: (111)–(111), (111)–(100), and (100)–(100). We computed the interaction energy for these pairs of facets facing each other for two identical nanocrystals of size N = 6181 in vacuum using the Sutton–Chen potential. The calculated potential energy curves shown in Fig. 5b indicate that, for all three facet combinations, two silver nanoparticles attract each other and come into contact without any energy barriers, consistent with the study by Schapotschnikow *et al.*,[36] such that silver nanocrystals in solution will rapidly aggregate. Note that in Fig. 5b, the potential energy is plotted as a function of the center-of-mass distance between the two closest facets of the two nanoparticles. The potential energies reach their minimum values at a distance of around 2.5 Å, when the silver atoms on the two facets are essentially in contact. Based on the nanoparticle coalescence mechanism given in previous studies of other researchers, [37,38] the silver nanoparticles will coagulate and rotate with respect to each other until their crystal orientation coincides.

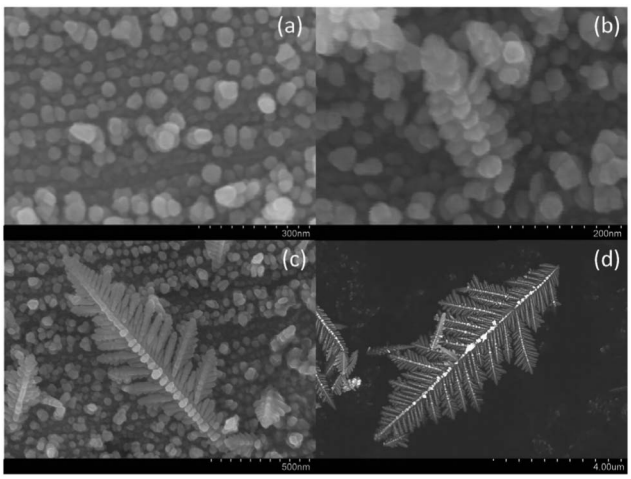

Fig. 6 Intermediate steps of the nanoparticle-based growth of a silver crystal at (a) 2 s, (b) 5 s, (c) 15 s, and (d) 35 s.

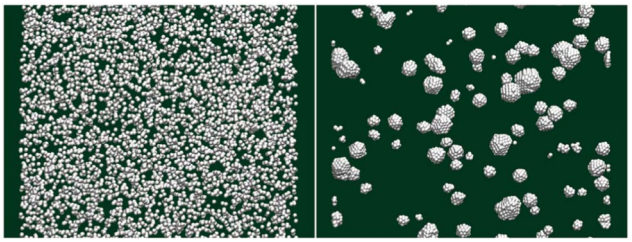

Fig. 7 (Left) Initial configuration with 6181 Ag atoms randomly distributed in a cubic simulation box. (Right) Nanocrystals formed by the Ag atoms after 40 ns of simulation time at 300 K.

Fig. 6 shows various stages of the formation of the dendritic structures as observed in our experiments. At the earliest stage of reaction, Ag ions were reduced to atoms and aggregated locally into nanoparticles with diameters between 10–30 nm within 2 seconds, as shown in Fig. 6a. During the next 5 seconds, the nanoparticles then diffused and attached to each other to grow into a corn-shaped rod with several columns of silver nanoparticles, as shown in Fig. 6b. As time went by for another 15 seconds, more nanoparticles connected to the rod from both ends to elongate the rod and from the sides to form branches that are similar to the entire structure, resulting in the dendritic structure in Fig. 6c. After 50 seconds, the dendritic structure grew into a larger one (Fig. 6d). Subsequent to the formation of the dendritic structure, more silver continued to attach and coagulate to the main body, finally forming a crystal (very likely to be a single crystal), such as the one shown in the right panel of Fig. 1.

An MD simulation was also performed to elucidate the initial stage of the formation of Ag nanoparticles when individual Ag atoms are reduced from the solution and start to coagulate. An initial configuration, shown in the left panel of Fig. 7, was prepared by placing 6181 Ag atoms at random positions in a periodic simulation cell with cubic geometry and a side length of 25 nm. A constant NVT simulation at T = 300 K with the Langevin dynamics (implicit water solvent with a damping coefficient of 14.35 ps^{-1}), carried out using the DL_POLY software package[29] with the silver atoms modeled by the Sutton–Chen force field,[30] was then performed for 40 ns and the final configuration is shown in the right panel of Fig. 7. Even in this short time, Ag atoms coagulated locally into many small faceted Ag nanoparticles. Therefore, in the experiments, Ag nanoparticles, rather than individual Ag atoms, should be the basic building blocks which form dendritic structures.

To explain the observed formation of dendritic structures we propose a growth mechanism based on the diffusion-limited aggregation theory[17] and the microscopic structure and interactions of the silver nanoparticles as basic building blocks. At the early stage of the reaction, individual Ag atoms are reduced from the solution and rapidly form small crystals. These crystals continue to grow, but the rate of diameter growth decreases quickly with time due to the reduced local density of silver atoms. At the same time, the formed

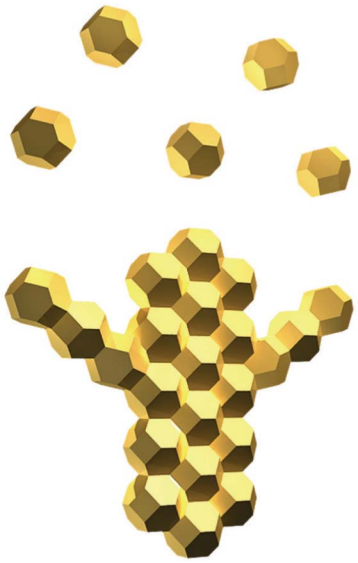

Fig. 8 Schematic illustration of the initial stage of the self-assembly process of silver nanoparticles.

nanoparticles also diffuse and assemble. The self-assembly of Ag nanoparticles dominates when they are sufficiently large and the growth rate of individual nanoparticles is very slow. In a self-assembly process without any energy barriers, the probability of a nanoparticle attaching to a certain facet of another particle is roughly proportional to the area of the facet S. Since for an ideal truncated octahedron, the ratio of the surface areas covered by (111) and (100) facets is $S111 : S100 \approx 3.5 : 1$, nanoparticles generally have a higher probability to attach to each other on (111) facets. Fig. 8 illustrates the schematic of an early stage of dendritic structure growth. After several nanoparticles attach to each other and grow into a rod, more particles join the two ends and elongate the stick. At the same time, some nanoparticles attach to the sides of the rod to form branches with a lower probability. Because in an ideal truncated octahedron the angle between the normals of two adjacent (111) facets is 70.5°, and the angle between the normals of two adjacent (111) and (100) facets is 54.8°, both close to 60°, the side branches always grow in the direction of about 60° with respect to their main branch as observed in our experiments. The main branches always grow longer than the side branches due to the larger stereo angles on two ends of branches than their sides. Dendritic structures form when the above mechanism is repeatedly applied to regulate the self-assembling growth of main and side branches at different levels. The spaces between branches are eventually filled up by more silver depositing on the structure and a single crystal is finally generated after a sufficiently long reaction time.

Conclusions

In summary, a non-equilibrium process of single crystal growth with self-assembled nanocrystals, rather than indivi-

dual atoms or ions, as basic building blocks has been observed in our experiments. The microscopic crystalline structure of these nanoparticles causes a dendritic structure to be formed *via* a multistep self-assembly process at intermediate stages of the growth process. This self-assembled nanostructure formation mechanism, which differs from the Ostwald ripening[24] and oriented attachment[25], may be useful for controlled crystal growth[39,40] which can yield crystals with designed structures and architectures for nanotechnological applications.

Acknowledgements

We thank Lisheng Zhang and Rui Shi for useful discussions. Funding by the Natural Science Foundation of Beijing (No. 2082006) and the National Natural Science Foundation of China (Grant No. 21073124), the Hundred Talent Program of the Chinese Academy of Sciences, and the Austrian Science Foundation (FWF) within the SFB ViCoM (F41), General program of science and technology development project of Beijing Municipal Education Commission (KM201010028005) and allocations of computer time from the Supercomputing Center in the Computer Network Information Center at the Chinese Academy of Sciences are gratefully acknowledged.

Notes and references

1 J. Aizenberg, A. J. Black and G. M. Whitesides, *Nature*, 1999, **398**, 495.
2 A. L. Briseno, S. C. B. Mannsfeld, M. M. Ling, S. Liu, R. J. Tseng, C. Reese, M. E. Roberts, Y. Yang, F. Wudl and Z. Bao, *Nature*, 2006, **444**, 913.
3 M. P. Hedges, J. J. Longdell, Y. Li and M. J. Sellars, *Nature*, 2010, **465**, 1052.
4 F. Huang, H. Zhang and J. F. Banfield, *Nano Lett.*, 2003, **3**, 373.
5 P. W. Atkins, in *Physical Chemistry*, W. H. Freeman & Co., New York, 1997.
6 J. Cahn, *Acta Metall.*, 1960, **8**, 554.
7 J. Cahn, W. Hillig and G. Sears, *Acta Metall.*, 1964, **12**, 1421.
8 J. Hilliard and J. Cahn, *Acta Metall.*, 1958, **6**, 772.
9 F. C. Frank, *Discuss. Faraday Soc.*, 1949, **5**, 48.
10 M. Volmer, in *Kinetic Der Phasenbildung*, Th. Steinkopf, Dresden, 1939.
11 W. K. Burton and N. Cabrera, *Discuss. Faraday Soc.*, 1949, **5**, 33.
12 W. K. Burton and N. Cabrera, *Discuss. Faraday Soc.*, 1949, **5**, 40.
13 W. K. Burton, N. Cabrera and F. C. Frank, *Philos. Trans. R. Soc. London, Ser. A*, 1951, **243**, 299.
14 N. Cabrera, *Discuss. Faraday Soc.*, 1959, **28**, 16.
15 K. A. Jackson, in *Growth and Perfection of Crystals*, ed. R. H. Doremus, B. W. Roberts and D. Turnbull, Wiley, New York, 1958.
16 T. M. Davis, T. O. Drews, H. Ramanan, C. He, J. Dong, H. Schnablegger, M. A. Katsoulakis, E. Kokkoli, A. V. McCormick, R. L. Penn and M. Tsapatsis, *Nat. Mater.*, 2006, **5**, 400.
17 T. A. Witten and L. M. Sander, *Phys. Rev. Lett.*, 1981, **47**, 1400.
18 H. Zheng, R. Smith, Y. Jun, C. Kisielowski, U. Dahmen and A. Alivisatos, *Science*, 2009, **324**, 1309.
19 L. Lu, A. Kobayashi, Y. Kikkawa, K. Tawa and Y. Ozaki, *J. Phys. Chem. B*, 2006, **110**, 23234.
20 X. Sun and M. Hagner, *Langmuir*, 2007, **23**, 9147.
21 X. Wen, Y. Xie, W. Mak, K. Cheung, X. Li, R. Renneberg and S. Yang, *Langmuir*, 2006, **22**, 4836.
22 C. Yan and D. Xue, *Cryst. Growth Des.*, 2008, **8**, 1849.
23 J. Ye, Q. Chen, H. Qi and N. Tao, *Cryst. Growth Des.*, 2008, **8**, 2464.
24 R. Theissmann, M. Fendrich, R. Zinetullin, G. Guenther, G. Schierning and D. E. Wolf, *Phys. Rev. B: Condens. Matter Mater. Phys.*, 2008, **78**, 205413.
25 J. Banfield, S. Welch, H. Zhang, T. Ebert and R. Penn, *Science*, 2000, **289**, 751.
26 G. MacBeath and S. L. Schreiber, *Science*, 2000, **289**, 1760.
27 R. F. Service, *Science*, 2001, **293**, 782.
28 J. Zhang, J. Liu, J. L. Huang, P. Kim and C. M. Lieber, *Science*, 1996, **274**, 757.
29 T. R. Forester and W. Smith, *Dl_Poly User Manual. CCLRC*, Daresbury Laboratory, Daresbury, Warrington, UK, 1995.
30 A. P. Sutton and J. Chen, *Philos. Mag. Lett.*, 1990, **61**, 139.
31 M. P. Allen and D. J. Tildesley, in *Computer Simulation of Liquids*, Oxford, Clarendon, 1987.
32 W. G. Hoover, *Phys. Rev. A*, 1985, **31**, 1695.
33 S. Nosé, *J. Chem. Phys.*, 1984, **81**, 511.
34 S. Ino, *J. Phys. Soc. Jpn.*, 1969, **27**, 941.
35 B. Wang, M. Liu, Y. Wang and X. Chen, *J. Phys. Chem. C*, 2011, **115**, 11374.
36 P. Schapotschnikow, R. Pool and T. J. H. Vlugt, *Nano Lett.*, 2008, **8**, 2930.
37 S. Arcidiacono, N. R. Bieri, D. Poulikakos and C. P. Grigoropoulos, *Int. J. Multiphase Flow*, 2004, **30**, 979.
38 E. Wong, J. Bonevich and P. Searson, *J. Phys. Chem. B*, 1998, **102**, 7770.
39 C. Hunziker, X. Zhan, P. A. Losio, H. Figi, O.-P. Kwon, S. Barlow, P. Guenter and S. R. Marder, *J. Mater. Chem.*, 2007, **17**, 4972.
40 D. Gu, H. Bongard, Y. Meng, K. Miyasaka, O. Terasaki, F. Zhang, Y. Deng, Z. Wu, D. Feng, Y. Fang, B. Tu, F. Schueth and D. Zhao, *Chem. Mater.*, 2010, **22**, 4828.

